Published in final edited form as:
Mol Pharm. 2013 May 6; 10(5): 1492–1504. doi:10.1021/mp300495e.

Diffusion of Macromolecules in the Brain: Implications for Drug Delivery

Daniel J. Wolak[1,2] and **Robert G. Thorne**[1,2,3,4,*]

[1]Pharmaceutical Sciences Division, University of Wisconsin-Madison School of Pharmacy, University of Wisconsin-Madison, Madison, WI 53705

[2]Clinical Neuroengineering Training Program, University of Wisconsin-Madison, Madison, WI 53705

[3]Neuroscience Training Program & Center for Neuroscience, University of Wisconsin-Madison, Madison, WI 53705

[4]Cellular and Molecular Pathology Graduate Training Program, University of Wisconsin-Madison, Madison, WI 53705

Abstract

Therapeutics must diffuse through the brain extracellular space (ECS) in order to distribute within the central nervous system (CNS) compartment; this requirement holds both for drugs that are directly placed within the CNS (i.e. central input) and for drugs that cross the barriers separating blood and brain following systemic administration. The diffusion of any substance within the CNS may be affected by a number of properties associated with the brain microenvironment, e.g. the volume fraction, geometry, width, and local viscosity of the ECS, as well as interactions with cell surfaces, the extracellular matrix, and components of the interstitial fluid. Here, we discuss ECS properties important in governing the distribution of macromolecules (e.g. antibodies and other protein therapeutics), nanoparticles and viral vectors within the CNS. We also provide an introduction to some of the methods commonly applied to measure diffusion of molecules in the brain ECS, with a particular emphasis on those used for determining the diffusion properties of macromolecules. Finally, we discuss how quantitative diffusion measurements can be used to better understand and potentially even improve upon CNS drug delivery by modeling delivery within and across species, screening drugs and drug conjugates, evaluating methods for altering drug distribution, and appreciating important changes in drug distribution that may occur with CNS disease or injury.

Keywords

Drug Delivery; Central Nervous System; Diffusion; Macromolecules; Proteins; Distribution; Extracellular Space

[*]Corresponding Author: Robert Thorne Ph.D., Pharmaceutical Sciences Division, University of Wisconsin-Madison School of Pharmacy, 5113 Rennebohm Hall, 777 Highland Avenue, Madison, WI 53705-2222, TEL: +1 608 890 3508. rthorne@wisc.edu.

Author Contributions

The manuscript was written through contributions of all authors. All authors have given approval to the final version of the manuscript.

Introduction

Central nervous system (CNS) disorders affect up to 1 billion people worldwide, accounting for more hospitalizations than any other disease group.[1] In the United States alone, neurological illnesses and mental disorders affect well over 50 million people annually at a cost of over $650 billion. Notwithstanding the obvious need for better treatments, new CNS drugs have historically suffered from considerably lower success rates than those for non-CNS indications (e.g. only 7% of CNS drugs entering clinical development are eventually approved versus about 15% for other therapeutic areas)[2], a situation that has led some in industry to paradoxically shift resources away from research on CNS disorders. There are many reasons for the low success rates of CNS drugs, including our still incomplete understanding of the brain and its many functions, the organ's propensity for off target side effects, and a shortage of validated biomarkers for assessing therapeutic efficacy, but the key challenge in many cases is related to delivery.[3,4] Indeed, the ability to achieve consistent, targeted delivery to the CNS remains a major, largely unmet challenge in the application of numerous small molecule and biopharmaceutical drugs. Among the largest obstacles to effective CNS delivery are the blood-brain and blood-cerebrospinal fluid barriers, formed by tight junctions between brain endothelial and epithelial cells that limit the transfer of substances between the plasma and the interstitial or cerebrospinal fluids of the CNS.[5,6,7,8] Typically, only small, lipophilic drugs are able to passively diffuse across the blood-brain barrier (BBB) in normal, healthy adults and children, although limited transport of certain peptides and peptide analogs has also been reported.[9] Transport of the active form of most peptides, proteins, oligonucleotides, nanoparticles and viral vectors across the normal, healthy CNS barriers from the systemic circulation has often proven so restricted that sufficient interest remains in using invasive, direct methods of administration (central injections and infusions into the parenchyma or the cerebrospinal fluid within the ventricles or subarachnoid space) to target biopharmaceutical drugs to the CNS. Regardless of the method used to introduce a drug into the CNS, all drugs must diffuse some distance through the narrow extracellular spaces of the brain microenvironment to distribute and produce effects.

Before further describing the brain microenvironment, it is necessary to first make some general observations about brain structure, nomenclature and scale.[10, 11,12,13] The CNS is divided into gray and white matter. Gray matter contains the cell bodies (somas) of neurons and glia (e.g. astrocytes, microglia and oligodendrocytes) along with their processes. Cell bodies of neurons vary greatly in size, from 5 – 10 μm (e.g. granule cells of the cerebellum) up to ~100 μm in diameter (e.g. Betz cells of the primary motor cortex); they are typically much larger than neuronal processes (axons and dendrites, collectively referred to as neurites), which can be as small as 0.2 μm. Glial cells vary greatly in size, particularly across species (e.g. the cell bodies and processes of human cortical protoplasmic astrocytes are several-fold larger than those in the rodent, with human astrocyte somas ~ 10 μm and their processes extending out 50 – 100 μm[14]). While somewhat controversial,[15] it is commonly held that glial cells outnumber neurons by as much as 2–10 times in the vertebrate forebrain,[13] although the glia:neuron ratio may vary markedly with brain size and among different CNS regions (e.g. there are greater than ten times more glia than neurons in the human thalamus and white matter but neurons greatly outnumber glia in the human cerebellum[16,17]). It is clear that glia take part in a vast number of CNS functions including blood flow regulation, metabolism, homeostasis and immune defense[18]; these cells are highly diversified in both form and function with this complexity increasing through evolution.[13–14, 18] The term neuropil is often used to refer to that portion of gray matter devoid of cell bodies, best appreciated in thin sections visualized by transmission electron microscopy (EM), where a dense arrangement of dendrites, axons (myelinated and unmyelinated) and glial processes can be seen (Figure 1).[10] It is apparent from electron

micrographs that the majority of the parenchyma in the gray matter consists of neuropil. White matter lacks neuronal cell bodies and consists primarily of axons ensheathed by the whitish-appearing myelin of oligodendrocytes.

Regardless of whether one examines an electron micrograph of gray or white matter, the brain microenvironment appears very densely packed with little space between cellular processes. Indeed, it is easy to overlook the brain extracellular space (ECS) in many conventionally prepared electron micrographs because the procedures used in preparing tissue sections from live animals are not ideal for preserving brain ECS fluid (also called interstitial fluid).[19] However, a variety of different methods better suited to the study of the brain microenvironment *in vivo* have all shown that the ECS occupies about 20% of the total tissue volume in most brain areas of normal, adult animals.[20,21,22] This important space is obviously critical to the distribution of neurotransmitters, nutrients, and all drugs within the CNS. Diffusion is an essential mechanism for the extracellular transport of most substances through the brain ECS; it is a process that is extremely fast and efficient over short distances such as the synaptic cleft (approximately 15 nm[10]) and it works quite well even for distances spanning a few cell bodies (distances of ~ 10 – 100 μm) but it can be very slow and limiting over the larger distances (~ mm and greater) often necessary for the effective distribution of drugs into the brain from its surfaces or from a syringe placed directly within one of its many regions. Neurons are rarely further than ~10–20 μm from their closest neighboring brain capillary (microvessel) in both rats[23] and primates[24] likely because the efficient diffusion of O_2, nutrients (e.g. glucose) and other molecules into the brain across the BBB has necessitated such organization. Diffusion is critically important in the CNS during its development, e.g. in the formation of morphogen gradients at the time of embryogenesis, and for its basic function, e.g. in the transfer of chemical signals from one neuron to another during neurotransmission. Neurons communicate with each other by the use of synapses. A presynaptic site (axon terminal) releases neurotransmitter into the synaptic cleft to interact with receptors on the postsynaptic site (typically, a dendrite) to open ion channels or to initiate a signaling cascade. In order for this sequence to occur with the correct spatial and temporal characteristics, neurotransmitter must rapidly diffuse across the synaptic cleft to reach certain postsynaptic receptors at a sufficiently high concentration and then be removed or deactivated so the steps may be repeated a short time later. There are major efforts to more accurately model the diffusion, spillover, binding, uptake, and crosstalk of neurotransmitters at the synaptic level in order to better understand neurotransmission.[25,26,27,28,29,30] During embryogenesis, morphogens affect CNS development through the establishment and shaping of their concentration gradients, a process greatly influenced by their extracellular diffusion. Experimental manipulation and modeling of these morphogen gradients is a major focus of study that has emphasized the potential importance of diffusion in the development of the brain and the whole organism.[31]

In this review, we introduce properties of the brain ECS and aspects of extracellular diffusion within the brain that are important to consider for CNS drug delivery. We also provide a brief overview of some of the main methods that have been used to measure extracellular diffusion within the brain and important findings that have resulted from these methods. Finally, we discuss how diffusion measurements can assist in better understanding, predicting and optimizing CNS delivery and distribution of therapeutics, particularly macromolecule biopharmaceutical drugs, for the treatment of neurological disorders.

Important Brain Extracellular Space Parameters

Brain ECS is sometimes imagined as the liquid phase of a foam, with the gaseous (air) phase equivalent to brain cells.[32] In reality, the shape and composition of the brain ECS is more complex. Looking at an electron micrograph of a small section of cortical neuropil shows

the ECS as a tortuous, snaking path separated by cell bodies and processes having many different sizes and shapes (Figure 1). The earliest EM studies had difficulty finding sufficient evidence of any ECS in the brain[33] because the manner in which tissue samples were obtained subjected the tissue to both ischemia and harsh processing; we now know ischemia induces significant cell swelling at the expense of the ECS (i.e. interstitial fluid water rapidly redistributes from the ECS into the intracellular compartment) and that subsequent fixation and drying of the tissue may further complicate the picture. [19,34, 35,36] Later EM work employed better preparative methods, consistently yielding a small but noticeable brain ECS, estimated to occupy about 5% of the total tissue volume on average[37] but the effect of ischemia remained. More specialized EM methods (rapid freezing followed by freeze substitution), better suited to preserving the extracellular fluid volume, suggested the ECS occupied a much larger percentage of total brain volume.[19,38] Physiological evidence, e.g. examination of the brain space occupied by endogenous molecules predominantly confined to the ECS (e.g. sodium and chloride ions) and results from the careful measurement of the spread of diffusible substances (i.e. diffusion measurements; discussed below) or the spread of current (impedance measurements) within the brain, also suggested the normal brain ECS volume was substantially greater than 5%.[20,39] Today, we know that the volume fraction of the brain ECS (α = ECS volume/total tissue volume) is about 0.2 (i.e. ECS accounts for about 20% of the total tissue volume) in most brain regions of normal, adult animals across multiple species. [20,39] Diffusion measurements have proven the most helpful in the routine measurement of α, yielding many insights into how this parameter changes over the lifespan in health and disease. For example, diffusion measurements in rodents have shown brain ECS volume is much larger in the early postnatal period immediately following birth ($\alpha \sim 0.4$), that ECS volume declines somewhat with advancing age ($\alpha \sim 0.13$–0.16 in 17–25 month old mice), and that CNS disease/injury models can dramatically change the situation (e.g. $\alpha \sim 0.05$ just minutes after severe ischemia). [36,40, 41]

Many EM studies that examined the volume of brain ECS also attempted to put a number to the average width or diameter of the intercellular spaces (d_{ECS}), usually reporting a range between ~10–20 nm.[19,37] Brain ECS width is of obvious importance for drug delivery because it may be regarded as providing an ‘upper limit’ for the size of a drug or vector that might be expected to distribute extracellularly within the neuropil. As with the ECS volume, it has long been appreciated that the brain ECS width visualized in most conventionally prepared electron micrographs likely underestimates the true dimensions in living tissue. These dimensions may fluctuate somewhat but recent *in vivo* diffusion measurements obtained in normal, adult rat neocortex have now established that a sufficient amount of well-connected ECS has an actual width averaging between 38–64 nm.[42] This estimate of d_{ECS} was derived by applying hydrodynamic theory for hindered diffusion (also called restricted diffusion theory) to quantitative diffusion data obtained in normoxic tissue for several dextrans (branched polymers of glucose) and inert quantum dot conjugates. Interestingly, applying this same theory to diffusion data obtained after terminal ischemia confirmed that the ECS width dropped to less than 10 nm under tissue conditions similar to that preceding preparation for EM.[42]

Brain ECS is filled with extracellular (interstitial) fluid containing an amorphous, negatively charged extracellular matrix (ECM) thought to play diverse roles in neural development, regeneration and signaling.[43] Brain ECM also serves as a dynamic, highly adaptable extracellular scaffold and key regulator of the diffusion of extracellular and membrane-associated molecules.[44,45] Normal brain ECM is thought to consist of a mesh-like network formed around a backbone of hyaluronic acid, a large, highly hydrated nonsulfated glycosaminoglycan; other important components include the heparan sulfate and chondroitin sulfate proteoglycans (HSPG and CSPG, respectively) along with an assortment of

glycoproteins, laminins and collagens. Among the more important ECM structures in the brain are perineuronal nets, consisting of aggregates of proteoglycans that surround the soma and proximal dendrites of neurons, and the basal lamina between brain endothelial cells and astrocyte foot processes at the BBB.[45] ECM components may be either bound to cells, e.g. by integrins, or free floating within the ECS.[46] Brain ECM could potentially affect the extracellular diffusion of endogenous molecules or drugs by a number of mechanisms, e.g. by increasing interstitial viscosity (slowing diffusion), by regulating the width and/or geometry of the ECS, or by the repulsion, attraction, transient binding or sequestration of ions or other charged substances.[22,44] A schematic diagram of the brain microenvironment depicting the narrow, tortuous ECS and the possible structural contributions of the ECM to the extracellular paths taken by diffusing substances is shown in Figure 2.

It is generally accepted among physiologists that little if any appreciable bulk flow (convection) of fluid is likely to occur within the ECS of the neuropil under normal conditions.[47,48,49] Indeed, transport measurements within brain parenchyma have mostly agreed rather well with basic diffusion theory without need for any modifications accounting for flow.[22,50] The transport of mass within a fluid is usually described in terms of a flux (the number of particles passing through a unit area per unit time); total flux may be divided into a diffusive component (always present so long as the particles are allowed the freedom to move) and a convective component (present when a volume containing the particles is moving with a certain velocity).[51] Diffusion is caused by random molecular movements, i.e. Brownian motion or random walks, that result in the net flux of particles from regions of higher to lower concentration; diffusive flux is directly proportional to the diffusion coefficient according to Fick's first law.[52] Convection typically refers to a flow driven by a pressure difference. According to Darcy's law, convective flux is directly proportional to the hydraulic permeability, a property describing the ease with which fluid flows through a material's pores; this property depends on features of both the convecting fluid and the material through which it must flow. The intrinsic hydraulic permeability, a component of the hydraulic permeability that describes the influence of the material's features (pore size, shape, tortuosity and availability), varies directly with the square of the mean pore diameter.[53] Experimental observations of convection within the brain have mostly been limited to lower resistance pathways (i.e. those expected to have a relatively higher intrinsic hydraulic permeability than the neuropil) such as the perivascular spaces of the cerebrovasculature, the white matter and the ventricular system.[47,48,49,54] There is much interest in the possibility that perivascular spaces, fluid-filled channels surrounding arteries, arterioles, veins, venules and possibly even microvessels, offer potential pathways for rapid flow into and out of brain parenchyma. Measurements of perivascular space widths in mammals suggest their typical dimensions may be at least two orders of magnitude greater than the neocortical ECS width (e.g. arteriole perivascular spaces have been reported in the range of ~5–10 μm or larger (in rodents and humans)[54,55,56] while the rat ECS width has been reported in the range of ~40–60 nm[42]); it follows that the intrinsic hydraulic permeability of the perivascular space might then be at least ~10,000-fold higher than the ECS of the neuropil. In other words, while some distribution of a drug or other substance by interstitial fluid flow within perivascular spaces of the parenchyma is likely both on theoretical grounds and from recent experimental observations,[54] further transport into the neuropil from this perivascular compartment is expected to be predominantly diffusive in nature (i.e. driven by the drug or substance's concentration gradient).

It is beyond the scope of this review to discuss details of the theory[21] underlying the description and analysis of diffusion in the brain ECS. At the microscopic scale, diffusion in a free solution of water or brain ECS is fundamentally driven by the kinetic energy of individual diffusing particles and their collisions with water molecules.[52,57] Fick's second law (often referred to as the macroscopic diffusion equation) describes how the time rate of

change in concentration ($\partial C/\partial t$) is equal to the product of the aqueous free diffusion coefficient (D) and the second spatial derivative of concentration ($\nabla^2 C$); modification of this relationship to describe how concentration changes with time in brain ECS (assuming bulk flow to be negligible) takes into account the porosity of brain tissue as well as how a diffusing substance is introduced into the brain and any loss or clearance that may occur[21,22]:

$$\frac{\partial C}{\partial t}=\frac{D}{\lambda^2}\cdot\nabla^2 C+\frac{Q}{\alpha}-\frac{f(C)}{\alpha} \quad \text{(Equation 1)}$$

The first term on the right-side of Eq. 1 accounts for diffusion in brain ECS. It contains the tortuosity (λ), a dimensionless parameter that describes the hindrance experienced by substances diffusing within the ECS relative to their diffusion in free solution (water or very dilute agarose):

$$\lambda=\sqrt{\frac{D}{D^*}} \quad \text{(Equation 2)}$$

This useful relationship allows us to easily introduce the effective diffusion coefficient in brain ECS (D^*; = D/λ^2) into Eq. 1. Tortuosity is a composite parameter that allows us to appreciate the increased hindrance that a diffusing substance is subjected to due to the constraints associated with extracellular diffusion within the brain microenvironment. The reasons for this increased hindrance are under investigation but may include potential contributions from a number of factors: an increase in path length forced by the need to diffuse around cellular and extracellular obstacles, trapping or delay within dead-space microdomains, viscous drag and steric hindrance imposed by ECM structure and/or the finite ECS width, and the effects of charge and/or binding.[21,22,42,44,58] The second term on the right-side of Eq. 1 (Q/α) accounts for the introduction of a substance into brain ECS by a source such as a pressure pulse or iontophoresis and the last term ($f(C)/\alpha$) represents clearance, loss or uptake from the ECS. The various techniques for measuring diffusion in the brain ECS commonly utilize analytical solutions to Eq. 1 appropriate for the experimental conditions associated with each method; analysis simply involves fitting the appropriate solution to the experimentally determined concentration distributions.

Measuring diffusion in the brain

The earliest technique used to measure diffusion coefficients in brain was the radiotracer technique developed by Fenstermacher, Patlak and colleagues, also known as the ventriculo-cisternal perfusion method.[59,60,61,62] In this method, a radiolabeled molecule is perfused through the ventricles of an anesthetized animal for several hours, typically through the introduction of an infusing needle in one of the lateral ventricles and a withdrawing needle placed within the cisterna magna (Figure 3). At the experiment's completion, the animal is euthanized, and the brain is rapidly removed and typically frozen before taking samples at various depths from the ventricular surface to determine the concentration distribution in periventricular areas such as the caudate nucleus by radioisotope counting. The resulting concentration distribution is then fit by an appropriate solution to Eq. 1 to obtain D^* and α; similar measurements may be performed in samples of agar gel to obtain D so that λ may also be calculated.

The ventriculo-cisternal perfusion technique represented a pioneering advance because it was really the first, scientifically valid physiological method that allowed measurement of α, in addition to yielding valuable diffusion and clearance information. The most reliable

and easiest-to-interpret applications of this method involved molecules like sucrose (342 Da) that mostly stayed confined within the ECS; measurements with [^{3}H]-sucrose yielded a volume fraction of approximately 0.2 and a tortuosity of 1.5–1.6 in the caudate nucleus of both dogs and rabbits.[50] Inulin, a 5 kDa macromolecule, was also tested by this method and returned similar although not identical values;[59] variances in molecular weight values and possible molecular decomposition may have slightly affected the results.[22] A number of other molecules were also studied but the results were harder to interpret since many did not stay confined within the ECS as they diffused into the periventricular tissue. The radiotracer method offers a potential way to determine the diffusion coefficient of potentially any therapeutic due to its ability to use any molecule to which a radioisotope may be attached for measurements. However, the technique is also associated with some disadvantages such as a complex surgical preparation, higher accuracy often necessitating the historical use of animals with larger brains (e.g. dogs or monkeys), and the ability to only produce a single time point per animal.

Since its application and description over thirty years ago by the group of Charles Nicholson[39], the method of real-time iontophoresis (RTI) has steadily become the most widely-used technique for measuring extracellular diffusion and associated parameters such as α in brain tissue. The RTI method requires the fabrication and use of iontophoretic and ion-selective microelectrodes to respectively administer and measure the change in concentration of a diffusing ion over time across a short distance, typically somewhere between 50 – 200 μm (Figure 3). In utilizing the controlled iontophoretic application of ions at a specific point, an appropriate point source solution to Eq. 1 may then be fit to the concentration distribution recorded over time by the ion-selective microelectrodes to obtain the diffusion coefficient and volume fraction. A form of the RTI technique was actually first introduced in the 1970s to measure the extracellular diffusion of K^+ ions by Lux and Neher[63] but unappreciated factors mostly associated with the complexities of K^+ transport (uptake and spatial buffering) led them to incorrectly analyze the resulting data. Subsequent refinements to the analysis finally allowed the now familiar application of RTI with the 74 Da tetramethylammonium cation (TMA^+), resulting in the first successful RTI measurements of brain ECS diffusion parameters.[39] TMA^+ has been favored because it is a small ion that remains mostly extracellular and is not known to affect the physiological function of the local tissue at the typical concentrations employed. The RTI method matched with TMA^+ (RTI-TMA) was first used *in vivo* for diffusion measurements in the rat cerebellum, although it may potentially be used in any region of the brain *in vivo* or *in vitro* (e.g. with an acute slice preparation). Although the RTI method is limited to small, charged ions for which suitable ion-selective microelectrodes can be fabricated; it is incredibly versatile, allowing for repeated measurements over time and in different brain regions of a single animal. Importantly, application of the RTI method with a suitable diffusing ion such as TMA^+ yields the ECS volume fraction (α) and clearance/uptake information in addition to diffusion coefficients; early application of the method yielded values for α of about 0.2, providing confirmation of the earlier ventriculo-cisternal perfusion results. Further discussion of the RTI technique and a comprehensive review of the results obtained from it in different species, brain regions, and altered physiological states may be found elsewhere.[22]

The technique of integrative optical imaging (IOI) is among the most valuable methods in use today for measuring the extracellular diffusion of substances other than the small ions used with the RTI method. First described by Nicholson and Tao in the 1990s,[64,65] the IOI method uses epifluorescence imaging to measure diffusion over time within a small region of brain ECS (typically, spanning a few hundred 3ms) following the pressure ejection of a small volume of fluorescent particles (typically, on the order of 25–50 picoliters[66]), approximating a point source (Figure 3). The diffusing particles may either be inherently

fluorescent substances (e.g. fluorophores, naturally fluorescent proteins or quantum dots) or virtually any other substance provided that a fluorescent label may be conjugated to or stably embedded within it. This feature has allowed the IOI method to be used with a wide variety of substances, including polypeptide and protein macromolecules, various polymers and nanoparticles (Table 1). [42,44,67,68,69,70] Substances are pressure injected into either a dilute (0.3%) agarose gel (for free diffusion measurements) or into brain tissue (for D^* measurements). Diffusion is recorded by obtaining a time sequence of images following injection using an epifluorescent microscope and CCD camera; an appropriate point source solution to Eq. 1 may then be fit to the fluorescence intensity distributions of the recorded images to obtain the diffusion coefficient.[21,68] IOI was first used to study the diffusion of globular macromolecules such as dextrans[64] and albumins[67] in acute slices prepared from the rat brain. Other studies have measured the diffusion of linear polymer chains of Poly[N-(2-hydroxypropyl)methacrylamide][71] and the epidermal growth factor protein[68] in brain slices. Recently, IOI was adapted to measure diffusion *in vivo* using open cranial windows to access the somatosensory cortex of anesthetized rats, yielding diffusion coefficients for 3 and 70 kDa dextrans, an inert surface PEGylated quantum dot nanoparticle, and the 80 kDa iron-binding proteins lactoferrin and transferrin.[42,44] While these studies provided valuable new diffusion parameters for each molecule *in vivo*, they also provided new insights into brain ECS properties through the application of a multi-component model for tortuosity that allowed the first-ever prediction of living brain ECS width based on hydrodynamic theory for hindered diffusion (equivalent pore analysis)[42] and the first *in vivo* estimate of HSPG binding site density (~3.5 μM) associated with the ECM of brain ECS.[44] As discussed above, this model yielded an estimate of brain ECS width or diameter (d_{ECS}) of 38–64 nm in the living rat neocortex, depending on whether the ECS was modeled as planar or cylindrical pores; Hrabetova and colleagues more recently applied scaling and reptation theory to dextran measurements in the isolated turtle cerebellum to predict an ECS width of ~31 nm.[70] The effects of light scattering have so far limited IOI to accessible superficial regions of the brain *in vivo* (typically, measurements are made several hundred microns below the brain's pial surface). The primary advantages of the IOI technique include the ability to perform repeated diffusion measurements over time, the potential to make measurements across different brain regions of a single animal if acute brain slices are utilized, and the ability to select among a diverse variety of fluorescent chemicals, proteins and conjugates for use in the measurements. IOI also typically yields higher accuracy measurements, requires fewer animals, and allows the potential investigation of smaller, more discrete brain areas compared to the radiotracer technique.

While the radiotracer, real-time iontophoresis and integrative optical imaging techniques represent the most commonly used methods for performing quantitative measurements of extracellular diffusion in brain tissue, other techniques of course exist. Saltzman and colleagues have described a point source method similar to IOI in which two photon imaging was paired with pressure injection to yield new diffusion measurements for the 26.5 kDa nerve growth factor (NGF) protein and 70 kDa dextran.[72] This initial application of multiphoton point source diffusion measurements produced values for the diffusion of 70 kDa dextran in rat neostriatal brain slices in very good agreement with earlier results obtained in rat neocortical slices using the single photon method of IOI, providing validation of each method.[64,72] Subsequent studies using the multiphoton point source methodology for a similar protein to NGF (brain-derived neurotrophic factor (27 kDa)) in rat neostriatal slices[73] and recent diffusion measurements for a range of dextrans and quantum dots in murine hippocampal slices using another IOI-like methodology[74] exhibited some variability[69] and technical difficulties but nevertheless emphasize the utility of the point source paradigm for experimental diffusion studies. Another general technique that has been extensively explored by Verkman and colleagues for *in vivo* diffusion measurements in brain involves the monitoring of fluorescence recovery after photobleaching (FRAP) either

at the cortical surface[75,76,77] or in deeper regions using a microfiberoptic.[78,79] FRAP is a technique that was first developed to measure two-dimensional lateral diffusion in cell membranes.[80] According to this original description of FRAP, fluorescent molecules are first uniformly 'loaded' into a large area of interest and then an intense pulse of light is used to irreversibly photobleach a smaller spot of well-defined shape (typically, a circle); subsequent replenishment of fluorescence within the smaller spot is monitored as nearby unbleached molecules diffuse into the bleached area and diffusion theory is used to explicitly determine a diffusion coefficient from the recovery curves. The performance and interpretation of FRAP in a three-dimensional volume such as the brain has been complicated by a number of challenges, e.g. difficulties associated with uniform loading of the tissue, uncertainties about the precise bleaching distribution, potential reversible bleaching and other factors; further discussion and comment on the *in vivo* application of FRAP in brain may be found elsewhere.[22] Regardless of the particular technique used to measure diffusion, the hallmark of most successfully applied methods thus far has been careful initial validation using diffusion probes and conditions where the expected results are known with a high degree of certainty from either basic theoretical principles (e.g. from correlations that predict the free diffusion coefficients of proteins with well-defined structures and size profiles[68]) or data previously obtained with other well-established methods under precise, easily reproduced conditions (e.g. experimental free diffusion coefficients measured at a described temperature).

Implications for drug delivery

Macromolecules may be administered and targeted to the brain in many different ways.[3,81] As we have seen, solutions to Eq. 1 for a given experimental paradigm with known boundary conditions may be fit to distribution data to obtain diffusion coefficients; conversely, if we know D^* and have information about clearance, loss and/or uptake (typically, in the form of an efflux constant (k_e)), solutions to Eq. 1 may sometimes be used to quantitatively predict disposition for a given biopharmaceutical drug within the CNS for a particular method of application. While the only way to know D^* for sure is to measure it directly, it has recently become possible to obtain rough estimates of D^* using model predictions for λ,[42] provided the apparent hydrodynamic diameter (d_H) is known or may be predicted; certain assumptions must also be made about whether substance transport will mainly be subject to steric interactions with ECS pores or further sources of hindrance (e.g. binding) may also be present.[44] For proteins > ~1 kDa, fairly good correlations exist for the prediction of d_H based on molecular weight, radius of gyration or ultracentrifugation data.[68] With d_H in hand, λ may be predicted using multi-component models of tortuosity, e.g. λ can be estimated using the ratio d_H/d_{ECS} when a diffusing substance is assumed to be relatively inert[42] (i.e. when other significant sources of hindrance such as binding to ECM components[44] or cellular receptors may be neglected at the concentrations considered). Once λ is predicted (and D is obtained from d_H using the Stokes-Einstein relationship[68]), D^* may be calculated using Eq. 2. A rough rule of thumb is that diffusional hindrance in brain ECS generally rises with increasing molecular weight (that is to say, λ gets larger and D^* decreases) so that large proteins, dextrans and nanoparticles nearly always exhibit λ values significantly greater than small molecules such as TMA^+ (where $\lambda \sim 1.5–1.6$ in most brain areas under normal conditions[22]); diffusion measurements in support of this relationship have been observed across multiple species and different laboratories.[42,68,70,72,74]

Once D^* is known or estimated for a given macromolecule or other substance and the k_e or efflux half-life ($t_{1/2} = \ln 2/k_e$) is determined by the brain efflux index[82] or other similar method[83], drug disposition may be modeled for central input under various conditions. For example, it is possible to model the concentration profile at steady state following continuous release from an interface held at a constant concentration (e.g. as might be the

case with continuous infusion into the CSF of the ventricles or subarachnoid space with no uptake by brain cells and neglecting any contribution from bulk flow[54]) using the appropriate solution to Eq. 1[21,68]:

$$\frac{C}{C_0} = e^{-x(k_e/D^*)^{1/2}} \quad \text{(Equation 3)}$$

Here, x is the distance from the interface surface (i.e. the ependymal surface of periventricular tissue or the pial brain surface facing the subarachnoid space), C is the concentration in the brain at distance x and C_0 is the concentration at either the periventricular or pial brain surface (i.e. $x = 0$); note that $C_0 = \alpha \cdot C_{csf}$ where α is the volume fraction (~0.2 in normal adults) and C_{csf} is the concentration in the CSF, i.e. the infusate concentration. Figure 4 shows the predicted concentration distributions from Eq. 3 for a small molecule (sucrose) and several different macromolecules using diffusion and efflux data summarized in Table 1. It can be appreciated how this sort of modeling may be informative when examining the results of a recent study by Scheule, Bankiewicz and colleagues in which recombinant human acid sphingomyelinase (ASM; ~70–75 kDa) was bilaterally infused into the lateral ventricles of rhesus monkeys and the resulting immunohistochemical distribution profile of ASM was obtained.[84] After a 4 h period of infusion, a gradient of ASM staining was mostly visible within the superficial 1–2 mm of tissue in direct contact with the subarachnoid space CSF (decreasing rapidly with distance away from the pial surface). This distribution of ASM is qualitatively similar to the profile predicted in Figure 4 for transferrin (an 80 kDa protein that does not bind ECM components appreciably) and lactoferrin (an 80 kDa protein for which significant binding to HSPG reduces D^*), proteins of similar molecular size to ASM, where C at a distance of 2 mm from the pial surface is predicted to be reduced ~100- to 1000-fold compared to C_0 (the concentration right at the pial surface). It is worth noting that the purely diffusive profiles shown in Figure 4 may not fully explain *in vivo* distribution profiles at all brain-CSF interfaces (e.g. convection within perivascular spaces may allow substances to distribute deeper and more broadly within the brain along penetrating blood vessels under some conditions[54] while a highly tortuous, multi-layered glia limitans formed by the processes of protoplasmic astrocytes may greatly restrict or even prevent diffusion across the pial surface in certain areas[85]); further research is needed to attain a more complete understanding of the complex factors at play when distribution into the brain from the CSF significantly deviates from the model predictions described here. As more reliable, quantitative diffusion and efflux data become available across an even wider variety of biopharmaceutical drugs, more accurate modeling, prediction and intelligent optimization may be possible for other methods, e.g. convection enhanced delivery or drug release from implanted polymer matrices.[86,87] The development of more accurate models may facilitate treatment of neurological disorders with macromolecules through more effective dosing, e.g. by allowing better estimation of CSF drug levels needed to penetrate and produce desired concentrations within specific brain regions.

The relative magnitude of the brain efflux constant k_e has a significant effect on CNS disposition, as may easily be appreciated by careful consideration of Eq. 3 and Fig. 4. Decreasing the k_e has long been a strategy for improving the time course and absolute level of drugs in the brain. The half-life of many systemic drugs can be improved through chemical modifications, e.g. peptide and protein drugs can be protected from degradation, rapid renal clearance, or unfavorable sequestration through the covalent attachment of polyethylene glycol chains (a process called PEGylation);[88,89] similar strategies have been proposed to enhance the disposition of CNS drugs following central input.[73] As chemical modifications such as PEGylation often change the size of macromolecule drugs, screening

the resulting conjugates for their diffusion behavior in brain has been shown to be a critical element in their rational design.[73] Antibodies offer another example of biopharmaceutical drugs whose disposition may be improved through modifications. By using modular forms of antibodies, e.g. smaller fragments of the antigen binding domain, it is possible to maintain specific targeting while greatly decreasing the size of the molecule. While use of a smaller antibody fragment often results in a decreased systemic half-life compared to full-length antibodies,[90,91,92] the decreased size of the fragments might be expected to result in increased penetration and distribution when released within the brain. Quantitative measurements using a technique such as IOI may be used to explicitly evaluate the diffusion characteristics of antibody fragments, perhaps in combination with other chemical modifications, providing a useful screen of their distribution potential in brain.

Since it is not always practical to change the structure of macromolecules, an alternative strategy for enhancing CNS disposition is the use of additives that improve extracellular transport either by eliciting a change in the brain microenvironment or through direct interactions with the diffusing substance. Many such strategies have involved the use of an osmolyte in an attempt to alter CNS fluid balance in a manner that favors increased drug disposition. It is well established from RTI-TMA diffusion measurements that osmotic stress such as that caused by the use of hypotonic or hypertonic solutions can dramatically affect α and λ.[93] An increase in α coupled with a decrease in λ could potentially explain the increased distribution of therapeutics such as adeno-associated viruses (AAV) when co-infused with hyperosmolar solutions of mannitol.[94,95] Heparin is a highly sulfated, strongly anionic glycosaminoglycan that binds with high affinity to proteins and other substances with putative heparin-binding regions. We have shown that lactoferrin, an 80 kDa protein containing a heparin-binding region, diffused significantly better in brain ECS when co-injected with heparin than when injected alone, a consequence of the relatively small and mobile exogenous heparin successfully competing against the normal association of lactoferrin with endogenous HSPG in the ECM.[44] Despite the larger size of the lactoferrin-heparin complex (~13 nm) compared to lactoferrin alone (~9 nm), diffusion in brain was significantly enhanced when binding to endogenous HSPG was reduced.[44] Other studies have observed increased distribution of substances with heparin binding regions (e.g. AAV[96] and GDNF[97]) when confused with heparin. It is obvious that most macromolecule drug candidates should experience some binding or uptake as part of their therapeutic action that may potentially limit their distribution. The concentration, location and affinity of these binding sites for a diffusing macromolecule would therefore be expected to influence both the therapeutic activity and distribution of the macromolecule in the brain. For example, antibody engineering approaches allow the affinity of antigen binding to be optimized for improved targeting and delivery, a method that has been used to achieve better brain penetration for antibodies targeting a putative receptor-mediated transcytosis system at the BBB[98]; optimization of antigen affinity for antibodies directed at CNS antigens might also be expected to affect antibody distribution within the brain ECS under some conditions.

Much is known about how different types of pathology, e.g. ischemia, traumatic injury, glioma and various disease models, affect diffusion parameters measured using RTI with the small TMA^+ ion.[22] By contrast, very little information exists on the diffusion of macromolecules in pathological conditions. We do know that terminal ischemia dramatically reduces D^* for 3 kDa dextran to less than 10% of its normal value in adult neocortex within minutes of onset.[42] As we have discussed, the consequence of such a reduction in D^* would be expected to result in markedly reduced drug disposition with almost any method of delivery. Several pathological states are associated with BBB abnormalities that may result in higher BBB permeability and presumably better CNS access for certain drugs[8]. However, increased CNS access due to higher BBB permeability may be offset somewhat by decreased ECS transport for conditions where the ECS volume fraction is significantly

lower than the normal adult value (0.2). Further measurements are required using methods such as IOI in combination with *in vivo* animal models of disease or injury to reveal precisely how different CNS pathological conditions may affect the diffusion of macromolecules and other biopharmaceutical drugs in brain ECS.

Finally, it is very important to appreciate that the CNS disposition of drugs that results from diffusive transport is not expected to change in species of different size. In other words, the same profile of decreasing concentration with distance shown in Figure 4 is expected whether we have delivered a macromolecule to the brain of a small animal or a human being. As already mentioned, measurements across many different brain regions in normal, adult species as diverse as fish, amphibians, reptiles and a range of mammals (rats, mice, guinea pigs, rabbits, dogs, and humans) have mostly yielded similar values for α (~ 0.2) and λ (~1.5–1.6) when small molecules have been used to evaluate diffusion in the ECS.[21,22] This feature suggests diffusion measurements for novel macromolecules and other biopharmaceutical drug candidates performed in commonly used species such as rats and mice will likely predict transport in human beings quite well. Furthermore, descriptive models of diffusive transport in the brain should also have great value across species. As El-Kareh and Secomb have eloquently stated:[99] “The key difference between a mouse and a man for some drugs is sometimes simply that the man is bigger but the drug still diffuses the same distance in a given time.”

This review has primarily focused on the implications of extracellular diffusion for the distribution of macromolecules, nanoparticles and viral vectors within the CNS. While these substances hold great promise for the treatment of a variety of CNS disorders, the great challenges associated with achieving effective CNS delivery have severely limited their clinical application; indeed, the only proteins that have been approved for clinical use in treating a neurological illness are those that act via peripheral mechanisms (e.g. type I interferons for treating multiple sclerosis). Achieving reliable, consistent CNS delivery for protein therapeutics and viral vectors for gene therapy would likely offer disease-modifying treatment options for many neurodegenerative diseases such as Alzheimer’s disease (e.g. antibodies for immunotherapy directed against beta-amyloid or gene therapy strategies utilizing transgenes for neurotrophic factors) and Parkinson’s disease (e.g. delivery of proteins or transgenes such as glial-cell line derived neurotrophic factor or neurturin) as well as in lysosomal storage diseases where systemically replaced enzymes are unable to access the CNS. Although intraparenchymal gene therapy approaches utilizing viral vectors are currently in clinical trials to treat CNS disorders[100] and intrathecal trials for lysosomal storage diseases have also begun[101], the achievement and prediction of consistent distributions between patients under different conditions has remained problematic. The application of monoclonal antibodies for use in Alzheimer’s disease are under evaluation in multiple large scale, late stage trials[102] but significant hurdles also remain for their clinical approval. Regardless of the approach used, successful clinical application of protein and gene therapies to treat brain disorders at their central target sites should benefit from novel strategies that incorporate new knowledge related to the barriers of the CNS, the physiology of the brain microenvironment, and transport processes within the brain’s interstitial and cerebrospinal fluids. This review has briefly summarized what is known about diffusion in the brain, a transport process with relevance for CNS drug delivery and distribution.

Acknowledgments

Funding Sources

This work was supported by the University of Wisconsin-Madison School of Pharmacy, the Graduate School at the University of Wisconsin, and the National Institute of Health (NRSA T32 EBO11424).

The authors thank Dr. Jeffery Lochhead and Mohan Gautum (University of Wisconsin-Madison) for reviewing the manuscript. RGT acknowledges (i) periodically receiving honoraria for speaking to organizations within academia, foundations, and the biotechnology and pharmaceutical industry and (ii) occasional service as a consultant on CNS drug delivery to industry.

References

1. [accessed Aug. 23, 2012] Brain Facts. http://www.brainfacts.org/
2. Pangalos MN, Schechter LE, Hurko O. Drug development for CNS disorders: strategies for balancing risk and reducing attrition. Nat Rev Drug Discov. 2007; 6(7):521–32. [PubMed: 17599084]
3. Thorne RG, Frey WH 2nd . Delivery of neurotrophic factors to the central nervous system: pharmacokinetic considerations. Clin Pharmacokinet. 2001; 40(12):907–46. [PubMed: 11735609]
4. Nagahara AH, Tuszynski MH. Potential therapeutic uses of BDNF in neurological and psychiatric disorders. Nat Rev Drug Discov. 2011; 10(3):209–19. [PubMed: 21358740]
5. Neuwelt E, Abbott NJ, Abrey L, Banks WA, Blakley B, Davis T, Engelhardt B, Grammas P, Nedergaard M, Nutt J, Pardridge W, Rosenberg GA, Smith Q, Drewes LR. Strategies to advance translational research into brain barriers. Lancet Neurol. 2008; 7(1):84–96. [PubMed: 18093565]
6. Abbott NJ, Patabendige AA, Dolman DE, Yusof SR, Begley DJ. Structure and function of the blood-brain barrier. Neurobiol Dis. 2010; 37(1):13–25. [PubMed: 19664713]
7. Pardridge WM. The blood-brain barrier: bottleneck in brain drug development. NeuroRx. 2005; 2(1):3–14. [PubMed: 15717053]
8. Neuwelt EA, Bauer B, Fahlke C, Fricker G, Iadecola C, Janigro D, Leybaert L, Molnar Z, O'Donnell ME, Povlishock JT, Saunders NR, Sharp F, Stanimirovic D, Watts RJ, Drewes LR. Engaging neuroscience to advance translational research in brain barrier biology. Nat Rev Neurosci. 2011; 12(3):169–82. [PubMed: 21331083]
9. Banks WA. Characteristics of compounds that cross the blood-brain barrier. BMC Neurol. 2009; 9(Suppl 1):S3. [PubMed: 19534732]
10. Peters, A.; Palay, SF.; Webster, HD. The Fine Structure of the Nervous System: Neurons and Their Supporting Cells. 3. Oxford University Press; New York: 1991.
11. Paxinos, G.; Mai, JK., editors. The Human Nervous System. Elsevier; Amsterdam: 2004.
12. Junqueria, LC.; Carneiro, J.; Kelly, RO. Basic Histology. Appleton & Large; Norwalk, CT: 1992.
13. Kandel, ER. Principles of neural science. 5. McGraw-Hill Medical; New York: 2013. p. 1p. 1709
14. Oberheim NA, Wang X, Goldman S, Nedergaard M. Astrocytic complexity distinguishes the human brain. Trends Neurosci. 2006; 29(10):547–53. [PubMed: 16938356]
15. Jabr, F. [accessed Dec. 14, 2012] Know Your Neurons: What Is the Ratio of Glia to Neurons in the Brain?. http://blogs.scientificamerican.com/brainwaves/2012/06/13/know-your-neurons-what-is-the-ratio-of-glia-to-neurons-in-the-brain/
16. Azevedo FA, Carvalho LR, Grinberg LT, Farfel JM, Ferretti RE, Leite RE, Jacob Filho W, Lent R, Herculano-Houzel S. Equal numbers of neuronal and nonneuronal cells make the human brain an isometrically scaled-up primate brain. J Comp Neurol. 2009; 513(5):532–41. [PubMed: 19226510]
17. Pelvig DP, Pakkenberg H, Stark AK, Pakkenberg B. Neocortical glial cell numbers in human brains. Neurobiol Aging. 2008; 29(11):1754–62. [PubMed: 17544173]
18. Oberheim NA, Goldman SA, Nedergaard M. Heterogeneity of astrocytic form and function. Methods Mol Biol. 2012; 814:23–45. [PubMed: 22144298]
19. Van Harreveld, A. The extracellular space in the vertebrate central nervous system. In: Bourne, GH., editor. The Structure and Function of Nervous Tissue. Vol. IV. Academic; New York: 1972. p. 447-511.
20. Nicholson C, Sykova E. Extracellular space structure revealed by diffusion analysis. Trends Neurosci. 1998; 21(5):207–15. [PubMed: 9610885]
21. Nicholson C. Diffusion and related transport mechanisms in brain tissue. Rep Prog Phys. 2001; 64(7):815–884.
22. Sykova E, Nicholson C. Diffusion in brain extracellular space. Physiol Rev. 2008; 88(4):1277–340. [PubMed: 18923183]

23. Schlageter KE, Molnar P, Lapin GD, Groothuis DR. Microvessel organization and structure in experimental brain tumors: microvessel populations with distinctive structural and functional properties. Microvasc Res. 1999; 58(3):312–28. [PubMed: 10527772]
24. Mabuchi T, Lucero J, Feng A, Koziol JA, del Zoppo GJ. Focal cerebral ischemia preferentially affects neurons distant from their neighboring microvessels. J Cereb Blood Flow Metab. 2005; 25(2):257–66. [PubMed: 15678127]
25. Rusakov DA, Kullmann DM. Extrasynaptic glutamate diffusion in the hippocampus: ultrastructural constraints, uptake, and receptor activation. J Neurosci. 1998; 18(9):3158–70. [PubMed: 9547224]
26. Rusakov DA, Savtchenko LP, Zheng K, Henley JM. Shaping the synaptic signal: molecular mobility inside and outside the cleft. Trends Neurosci. 2011
27. Vargova L, Sykova E. Extracellular space diffusion and extrasynaptic transmission. Physiol Res. 2008; 57(Suppl 3):S89–99. [PubMed: 18481911]
28. Coggan JS, Bartol TM, Esquenazi E, Stiles JR, Lamont S, Martone ME, Berg DK, Ellisman MH, Sejnowski TJ. Evidence for ectopic neurotransmission at a neuronal synapse. Science. 2005; 309(5733):446–51. [PubMed: 16020730]
29. Matsui K, Jahr CE, Rubio ME. High-concentration rapid transients of glutamate mediate neural-glial communication via ectopic release. J Neurosci. 2005; 25(33):7538–47. [PubMed: 16107641]
30. Kinney JP, Spacek J, Bartol TM, Bajaj CL, Harris KM, Sejnowski TJ. Extracellular sheets and tunnels modulate glutamate diffusion in hippocampal neuropil. J Comp Neurol. 2012
31. Briscoe, J.; Lawrence, PA.; Vincent, JP. Generation and Interpretation of Morphogen Gradients. Cold Spring Harbor Laboratory Press; Cold Spring Harbor, NY: 2010. p. 308
32. Kuffler SW, Potter DD. Glia in the Leech Central Nervous System: Physiological Properties and Neuron-Glia Relationship. J Neurophysiol. 1964; 27:290–320. [PubMed: 14129773]
33. Wyckoff RW, Young JZ. The motorneuron surface. Proc R Soc Lond B Biol Sci. 1956; 144(917): 440–50. [PubMed: 13310574]
34. Villegas GM, Fernandez J. Permeability to thorium dioxide of the intercellular spaces of the frog cerebral hemisphere. Exp Neurol. 1966; 15(1):18–36. [PubMed: 5934661]
35. Hansen AJ. Effect of anoxia on ion distribution in the brain. Physiol Rev. 1985; 65(1):101–48. [PubMed: 3880896]
36. Vorisek I, Sykova E. Ischemia-induced changes in the extracellular space diffusion parameters, K +, and pH in the developing rat cortex and corpus callosum. J Cereb Blood Flow Metab. 1997; 17(2):191–203. [PubMed: 9040499]
37. Horstmann E, Meves H. Die Feinstruktur des molekularen Rindengraues und ihre physiologische Bedeutung. Z Zellforsch. 1959; 49:569–604.
38. Trubatch J, Loud AV, Van Harreveld A. Quantitative stereological evaulation of KC1-induced ultrastructural changes in frog brain. Neuroscience. 1977; 2(6):963–974.
39. Nicholson C, Phillips JM. Ion diffusion modified by tortuosity and volume fraction in the extracellular microenvironment of the rat cerebellum. J Physiol. 1981; 321:225–57. [PubMed: 7338810]
40. Lehmenkuhler A, Sykova E, Svoboda J, Zilles K, Nicholson C. Extracellular space parameters in the rat neocortex and subcortical white matter during postnatal development determined by diffusion analysis. Neuroscience. 1993; 55(2):339–51. [PubMed: 8377929]
41. Sykova E, Vorisek I, Antonova T, Mazel T, Meyer-Luehmann M, Jucker M, Hajek M, Ort M, Bures J. Changes in extracellular space size and geometry in APP23 transgenic mice: a model of Alzheimer's disease. Proc Natl Acad Sci U S A. 2005; 102(2):479–84. [PubMed: 15630088]
42. Thorne RG, Nicholson C. In vivo diffusion analysis with quantum dots and dextrans predicts the width of brain extracellular space. Proc Natl Acad Sci U S A. 2006; 103(14):5567–72. [PubMed: 16567637]
43. Dityatev A, Schachner M. Extracellular matrix molecules and synaptic plasticity. Nat Rev Neurosci. 2003; 4(6):456–68. [PubMed: 12778118]
44. Thorne RG, Lakkaraju A, Rodriguez-Boulan E, Nicholson C. In vivo diffusion of lactoferrin in brain extracellular space is regulated by interactions with heparan sulfate. Proc Natl Acad Sci U S A. 2008; 105(24):8416–21. [PubMed: 18541909]

45. Dityatev A, Seidenbecher CI, Schachner M. Compartmentalization from the outside: the extracellular matrix and functional microdomains in the brain. Trends Neurosci. 2010; 33(11): 503–12. [PubMed: 20832873]
46. Novak U, Kaye AH. Extracellular matrix and the brain: components and function. J Clin Neurosci. 2000; 7(4):280–90. [PubMed: 10938601]
47. Abbott NJ. Evidence for bulk flow of brain interstitial fluid: significance for physiology and pathology. Neurochem Int. 2004; 45(4):545–52. [PubMed: 15186921]
48. Rosenberg GA, Kyner WT, Estrada E. Bulk flow of brain interstitial fluid under normal and hyperosmolar conditions. Am J Physiol. 1980; 238(1):F42–9. [PubMed: 7356021]
49. Ichimura T, Fraser PA, Cserr HF. Distribution of extracellular tracers in perivascular spaces of the rat brain. Brain Res. 1991; 545(1–2):103–13. [PubMed: 1713524]
50. Fenstermacher J, Kaye T. Drug "diffusion" within the brain. Ann N Y Acad Sci. 1988; 531:29–39. [PubMed: 3382143]
51. Weiss, TF. Cellular biophysics. MIT Press; Cambridge, Mass: 1996.
52. Berg, HC. Random Walks in Biology. Princeton University Press; Princeton, NJ: 1993.
53. Bear, J. Dynamics of fluids in porous media. American Elsevier Pub. Co; New York: 1972. p. xviip. 764
54. Iliff JJ, Wang M, Liao Y, Plogg BA, Peng W, Gundersen GA, Benveniste H, Vates GE, Deane R, Goldman SA, Nagelhus EA, Nedergaard M. A Paravascular Pathway Facilitates CSF Flow Through the Brain Parenchyma and the Clearance of Interstitial Solutes, Including Amyloid beta. Sci Transl Med. 2012; 4(147):147ra111.
55. Foley CP, Nishimura N, Neeves KB, Schaffer CB, Olbricht WL. Real-Time Imaging of Perivascular Transport of Nanoparticles During Convection-Enhanced Delivery in the Rat Cortex. Annals of Biomedical Engineering. 2012; 40(2):292–303. [PubMed: 22009318]
56. Pollock H, Hutchings M, Weller RO, Zhang ET. Perivascular spaces in the basal ganglia of the human brain: their relationship to lacunes. J Anat. 1997; 191(Pt 3):337–46. [PubMed: 9418990]
57. Hille, B. Ion channels of excitable membranes. 3. Sinauer: Sunderland, Mass; 2001. p. xviiip. 814
58. Hrabetova S, Hrabe J, Nicholson C. Dead-space microdomains hinder extracellular diffusion in rat neocortex during ischemia. J Neurosci. 2003; 23(23):8351–9. [PubMed: 12967997]
59. Levin VA, Fenstermacher JD, Patlak CS. Sucrose and inulin space measurements of cerebral cortex in four mammalian species. Am J Physiol. 1970; 219(5):1528–33. [PubMed: 4990676]
60. Patlak CS, Fenstermacher JD. Measurements of dog blood-brain transfer constants by ventriculocisternal perfusion. Am J Physiol. 1975; 229(4):877–84. [PubMed: 1190330]
61. Kessler JA, Fenstermacher JD, Owens ES. Spinal subarachnoid perfusion of rhesus monkeys. Am J Physiol. 1976; 230(3):614–8. [PubMed: 817608]
62. Rall DP, Oppelt WW, Patlak CS. Extracellular space of brain as determined by diffusion of inulin from the ventricular system. Life Science. 1962; 2:43–48.
63. Lux HD, Neher E. The equilibration time course of (K +) 0 in cat cortex. Exp Brain Res. 1973; 17(2):190–205. [PubMed: 4714525]
64. Nicholson C, Tao L. Hindered diffusion of high molecular weight compounds in brain extracellular microenvironment measured with integrative optical imaging. Biophys J. 1993; 65(6):2277–90. [PubMed: 7508761]
65. Tao L, Nicholson C. The three-dimensional point spread functions of a microscope objective in image and object space. J Microsc. 1995; 178(Pt 3):267–71. [PubMed: 7666411]
66. Cragg SJ, Nicholson C, Kume-Kick J, Tao L, Rice ME. Dopamine-mediated volume transmission in midbrain is regulated by distinct extracellular geometry and uptake. J Neurophysiol. 2001; 85(4):1761–71. [PubMed: 11287497]
67. Tao L, Nicholson C. Diffusion of albumins in rat cortical slices and relevance to volume transmission. Neuroscience. 1996; 75(3):839–47. [PubMed: 8951877]
68. Thorne RG, Hrabetova S, Nicholson C. Diffusion of epidermal growth factor in rat brain extracellular space measured by integrative optical imaging. J Neurophysiol. 2004; 92(6):3471–81. [PubMed: 15269225]

69. Thorne RG, Hrabetova S, Nicholson C. Diffusion measurements for drug design. Nat Mater. 2005; 4(10):713. author reply 714. [PubMed: 16195756]
70. Xiao F, Nicholson C, Hrabe J, Hrabetova S. Diffusion of flexible random-coil dextran polymers measured in anisotropic brain extracellular space by integrative optical imaging. Biophys J. 2008; 95(3):1382–92. [PubMed: 18456831]
71. Prokopova-Kubinova S, Vargova L, Tao L, Ulbrich K, Subr V, Sykova E, Nicholson C. Poly[N-(2-hydroxypropyl)methacrylamide] polymers diffuse in brain extracellular space with same tortuosity as small molecules. Biophys J. 2001; 80(1):542–8. [PubMed: 11159424]
72. Stroh M, Zipfel WR, Williams RM, Webb WW, Saltzman WM. Diffusion of nerve growth factor in rat striatum as determined by multiphoton microscopy. Biophysical Journal. 2003; 85(1):581–588. [PubMed: 12829512]
73. Stroh M, Zipfel WR, Williams RM, Ma SC, Webb WW, Saltzman WM. Multiphoton microscopy guides neurotrophin modification with poly(ethylene glycol) to enhance interstitial diffusion. Nature Materials. 2004; 3(7):489–494.
74. Scimemi A, Tian H, Diamond JS. Neuronal Transporters Regulate Glutamate Clearance, NMDA Receptor Activation, and Synaptic Plasticity in the Hippocampus (November, pg 14581; 2009). Journal of Neuroscience. 2010; 30(29):9954–9956.
75. Binder DK, Papadopoulos MC, Haggie PM, Verkman AS. In vivo measurement of brain extracellular space diffusion by cortical surface photobleaching. J Neurosci. 2004; 24(37):8049–56. [PubMed: 15371505]
76. Papadopoulos MC, Binder DK, Verkman AS. Enhanced macromolecular diffusion in brain extracellular space in mouse models of vasogenic edema measured by cortical surface photobleaching. FASEB J. 2005; 19(3):425–7. [PubMed: 15596484]
77. Papadopoulos MC, Kim JK, Verkman AS. Extracellular space diffusion in central nervous system: anisotropic diffusion measured by elliptical surface photobleaching. Biophys J. 2005; 89(5):3660–8. [PubMed: 16143636]
78. Thiagarajah JR, Kim JK, Magzoub M, Verkman AS. Slowed diffusion in tumors revealed by microfiberoptic epifluorescence photobleaching. Nat Methods. 2006; 3(4):275–80. [PubMed: 16554832]
79. Zador Z, Magzoub M, Jin S, Manley GT, Papadopoulos MC, Verkman AS. Microfiberoptic fluorescence photobleaching reveals size-dependent macromolecule diffusion in extracellular space deep in brain. FASEB J. 2008; 22(3):870–9. [PubMed: 17965267]
80. Axelrod D, Koppel DE, Schlessinger J, Elson E, Webb WW. Mobility measurement by analysis of fluorescence photobleaching recovery kinetics. Biophys J. 1976; 16(9):1055–69. [PubMed: 786399]
81. Lochhead JJ, Thorne RG. Intranasal delivery of biologics to the central nervous system. Adv Drug Deliv Rev. 2012; 64(7):614–28. [PubMed: 22119441]
82. Kakee A, Terasaki T, Sugiyama Y. Brain efflux index as a novel method of analyzing efflux transport at the blood-brain barrier. J Pharmacol Exp Ther. 1996; 277(3):1550–9. [PubMed: 8667222]
83. Groothuis DR, Vavra MW, Schlageter KE, Kang EW, Itskovich AC, Hertzler S, Allen CV, Lipton HL. Efflux of drugs and solutes from brain: the interactive roles of diffusional transcapillary transport, bulk flow and capillary transporters. J Cereb Blood Flow Metab. 2007; 27(1):43–56. [PubMed: 16639426]
84. Ziegler RJ, Salegio EA, Dodge JC, Bringas J, Treleaven CM, Bercury SD, Tamsett TJ, Shihabuddin L, Hadaczek P, Fiandaca M, Bankiewicz K, Scheule RK. Distribution of acid sphingomyelinase in rodent and non-human primate brain after intracerebroventricular infusion. Exp Neurol. 2011; 231(2):261–71. [PubMed: 21777586]
85. Ghersi-Egea JF, Finnegan W, Chen JL, Fenstermacher JD. Rapid distribution of intraventricularly administered sucrose into cerebrospinal fluid cisterns via subarachnoid velae in rat. Neuroscience. 1996; 75(4):1271–1288. [PubMed: 8938759]
86. Powell EM, Sobarzo MR, Saltzman WM. Controlled release of nerve growth factor from a polymeric implant. Brain Res. 1990; 515(1–2):309–11. [PubMed: 2357568]

87. Saltzman WM, Radomsky ML. Drugs Released from Polymers - Diffusion and Elimination in Brain-Tissue. Chem Eng Sci. 1991; 46(10):2429–2444.

88. Jain A, Jain SK. PEGylation: an approach for drug delivery. A review. Crit Rev Ther Drug Carrier Syst. 2008; 25(5):403–47. [PubMed: 19062633]

89. Harris JM, Chess RB. Effect of pegylation on pharmaceuticals. Nat Rev Drug Discov. 2003; 2(3): 214–21. [PubMed: 12612647]

90. Nelson AL. Antibody fragments: hope and hype. MAbs. 2010; 2(1):77–83. [PubMed: 20093855]

91. Yokota T, Milenic DE, Whitlow M, Schlom J. Rapid tumor penetration of a single-chain Fv and comparison with other immunoglobulin forms. Cancer Res. 1992; 52(12):3402–8. [PubMed: 1596900]

92. Jain RK. Physiological barriers to delivery of monoclonal antibodies and other macromolecules in tumors. Cancer Res. 1990; 50(3 Suppl):814s–819s. [PubMed: 2404582]

93. Kume-Kick J, Mazel T, Vorisek I, Hrabetova S, Tao L, Nicholson C. Independence of extracellular tortuosity and volume fraction during osmotic challenge in rat neocortex. J Physiol. 2002; 542(Pt 2):515–27. [PubMed: 12122149]

94. Burger C, Nguyen FN, Deng J, Mandel RJ. Systemic mannitol-induced hyperosmolality amplifies rAAV2-mediated striatal transduction to a greater extent than local co-infusion. Mol Ther. 2005; 11(2):327–31. [PubMed: 15668145]

95. Mastakov MY, Baer K, Xu R, Fitzsimons H, During MJ. Combined injection of rAAV with mannitol enhances gene expression in the rat brain. Mol Ther. 2001; 3(2):225–32. [PubMed: 11237679]

96. Mastakov MY, Baer K, Kotin RM, During MJ. Recombinant adeno-associated virus serotypes 2- and 5-mediated gene transfer in the mammalian brain: quantitative analysis of heparin co-infusion. Mol Ther. 2002; 5(4):371–80. [PubMed: 11945063]

97. Hamilton JF, Morrison PF, Chen MY, Harvey-White J, Pernaute RS, Phillips H, Oldfield E, Bankiewicz KS. Heparin coinfusion during convection-enhanced delivery (CED) increases the distribution of the glial-derived neurotrophic factor (GDNF) ligand family in rat striatum and enhances the pharmacological activity of neurturin. Exp Neurol. 2001; 168(1):155–61. [PubMed: 11170730]

98. Yu YJ, Zhang Y, Kenrick M, Hoyte K, Luk W, Lu Y, Atwal J, Elliott JM, Prabhu S, Watts RJ, Dennis MS. Boosting brain uptake of a therapeutic antibody by reducing its affinity for a transcytosis target. Sci Transl Med. 2011; 3(84):84ra44.

99. El-Kareh AW, Secomb TW. Theoretical models for drug delivery to solid tumors. Crit Rev Biomed Eng. 1997; 25(6):503–571. [PubMed: 9719859]

100. Lim ST, Airavaara M, Harvey BK. Viral vectors for neurotrophic factor delivery: a gene therapy approach for neurodegenerative diseases of the CNS. Pharmacol Res. 2010; 61(1):14–26. [PubMed: 19840853]

101. Dickson PI, Chen AH. Intrathecal enzyme replacement therapy for mucopolysaccharidosis I: translating success in animal models to patients. Curr Pharm Biotechnol. 2011; 12(6):946–55. [PubMed: 21506913]

102. Robert R, Wark KL. Engineered antibody approaches for Alzheimer's disease immunotherapy. Arch Biochem Biophys. 2012; 526(2):132–8. [PubMed: 22475448]

103. Zhang Y, Pardridge WM. Mediated efflux of IgG molecules from brain to blood across the blood-brain barrier. J Neuroimmunol. 2001; 114(1–2):168–72. [PubMed: 11240028]

104. Cserr HF, Cooper DN, Suri PK, Patlak CS. Efflux of radiolabeled polyethylene glycols and albumin from rat brain. Am J Physiol. 1981; 240(4):F319–28. [PubMed: 7223889]

105. Zhang Y, Pardridge WM. Rapid transferrin efflux from brain to blood across the blood-brain barrier. J Neurochem. 2001; 76(5):1597–600. [PubMed: 11238745]

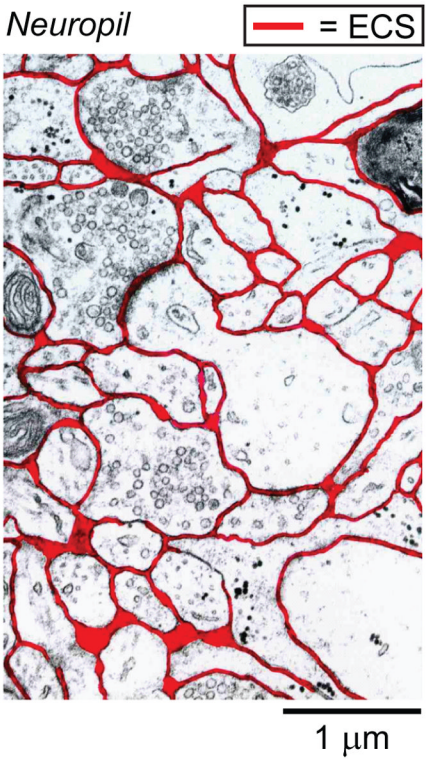

Figure 1.
Electron micrograph showing a small area of cortical neuropil from the brain of a rat. The ECS has been roughly outlined by hand in red. A typical synapse is shown between a presynaptic neuronal terminal (with clear, round vesicles containing neurotransmitter) and a dendritic spine of a postsynaptic neuron (displaying a dark electron-dense region called the postsynaptic density) - a narrow synaptic cleft may be identified between them. Adapted with permission from Nicholson and Sykova (1998).

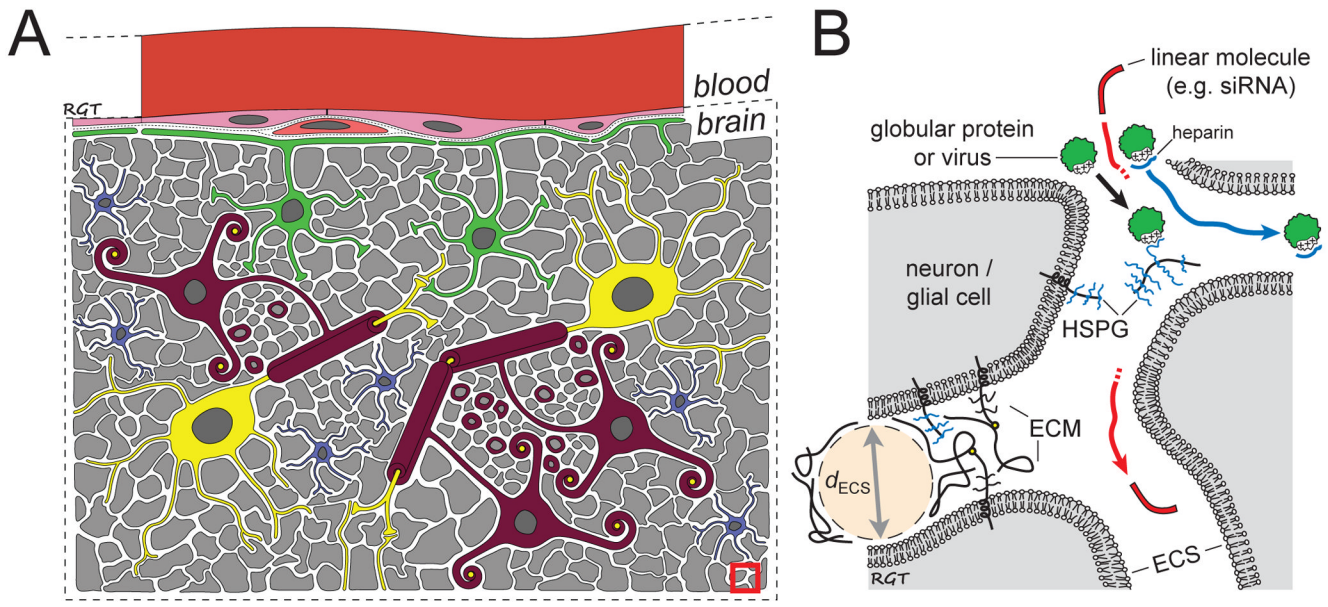

Figure 2.

Schematic of the brain microenvironment emphasizing the importance of the extracellular space (ECS) in the diffusion of drugs. A) The brain microenvironment is a crowded space packed with many different types of cells: astrocytes (green), oligodendrocytes (maroon), neurons (yellow), and microglia (blue). Brain endothelial cells (pink) and pericytes (light red) are associated with the brain microvessels. Neurites (axonal and dendritic processes or neurons) and glial processes making up the neuropil are shown in grey. Regardless of whether a drug or other substance crosses the blood-brain barrier or is directly applied within the brain, distribution within the brain microenvironment usually must involve diffusion over some distance within the brain ECS. B) Schematic showing a magnified view of the red box in A. ECS width (d_{ECS}) and extracellular matrix (ECM) components such as heparan sulfate proteoglycans (HSPG) may influence the diffusion of biologic drugs having either globular (e.g. proteins or viral vectors) or linear configurations (e.g. short interfering RNA (siRNA)). The diffusion of proteins and viruses that bind HSPG may be enhanced by complexation with heparin, preventing association with endogenous HSPG.[44]

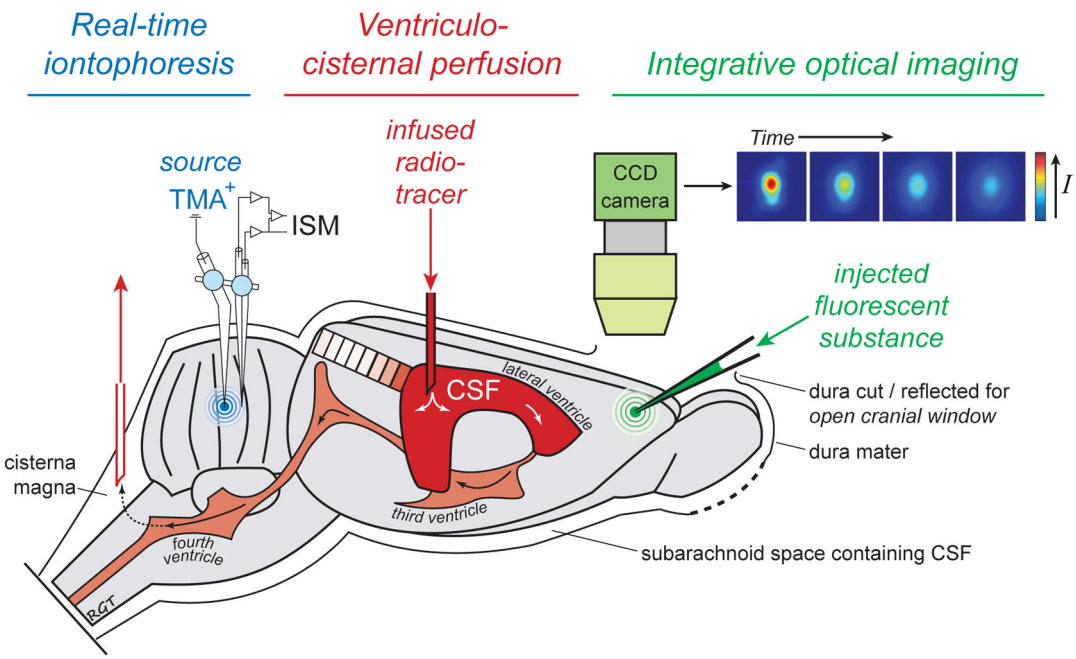

Figure 3.

Methods of measuring extracellular diffusion coefficients and other important ECS parameters in brain tissue. Real-time iontophoresis is a technique that employs iontophoresis of small ions, typically the 74 Da tetramethylammonium (TMA) cation, from a source microelectrode and the subsequent measurement of the resulting local concentration over time some short distance away from the release site by an ion-selective microelectrode. The real-time iontophoretic technique is useful because it potentially can be applied to any brain region, although it has typically been limited to small, charged ions for which suitable ion-selective microelectrodes can be fabricated. Particular strengths of the real-time iontophoretic method are that it can be performed repeatedly in the same animal at different locations/time points and it yields the ECS volume fraction (α) and clearance/uptake information in addition to diffusion coefficients. The ventriculo-cisternal perfusion technique is used to measure transport into brain areas bordering the ventricular system (a modification of the method may also be used to measure transport across the brain's pial surface from the subarachnoid space). Typically, a radiotracer is infused into the cerebrospinal fluid (CSF) of the lateral ventricle and then removed from the cistern at an equivalent rate. After a suitable time, the brain is carefully removed and samples are taken to measure the radiotracer concentration at various depths; the resulting distribution may then be analyzed to yield 3, clearance information and diffusion coefficients. While the range of substances that may be explored using the ventriculo-cisternal perfusion method is broad, the complexity of the surgical preparation and difficulties associated with utilizing a radioactivity-based technique has limited its contemporary use; it also is only capable of producing a single time point per animal. Finally, integrative optical imaging is a technique in which a very small volume of fluid containing a fluorescently labeled substance is pressure-injected into the brain and the resulting concentration distribution is recorded over time using an epifluorescent microscope and CCD camera. Diffusion coefficients are obtained by fitting fluorescence intensity curves from the resulting images with the appropriate solution to the diffusion equation. While integrative optical imaging cannot easily be used to obtain 3 or clearance/uptake information, it is routinely employed to measure diffusion coefficients for a wide range of fluorescent substances and fluorophore-drug conjugates at multiple locations and time points within the same animal.

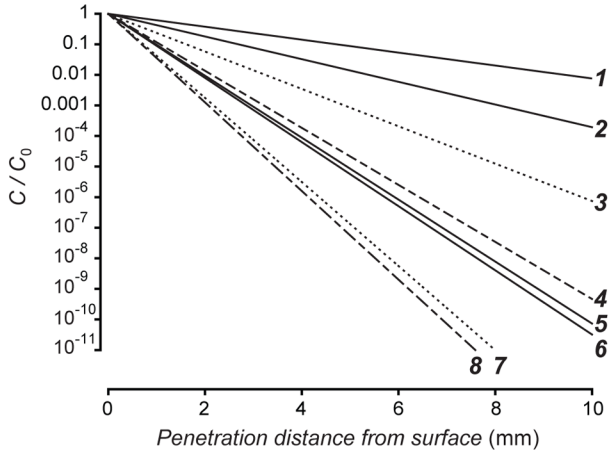

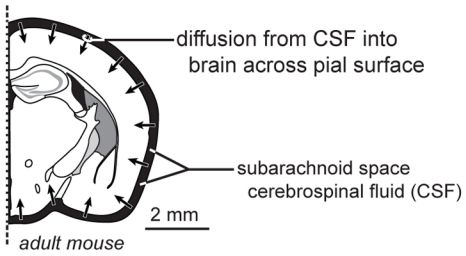

Molecule	*MW* (Da)	*hydrodynamic diameter* (d_H; nm)	*half-life in brain* ($t_{1/2}$; hr)	*predicted* C / C_0 (x = 2 mm)
1. Sucrose	342	0.9	2.6	0.38
2. Inulin	5000	2.7	2.3	0.18
3. Dextran*	70000	14	15	0.06
4. Transferrin	80000	8.8	2.8	0.012
5. NGF	26500	4.9	1.2	0.0094
6. BSA	66000	7.4	1.9	0.0080
7. Dextran*	70000	14	3.0	0.0018
8. Lactoferrin	80000	9.3	2.8	0.0011

Figure 4.

Modeling penetration into the brain from the cerebrospinal fluid (CSF). Predicted concentration profiles into brain tissue (left) resulting from intracerebroventricular or intrathecal input at steady state. Eq. 3 (see text for details) was used to predict C/C_0, the ratio of the concentration in the brain at a given penetration distance to the concentration at the periventricular or pial brain surface, from diffusion and efflux data in Table 1. Two different brain efflux constants are used for the 70 kDa dextran profiles (corresponding to a short half-life in brain of 3.0 hr[83] or a long half-life in brain of 15 hr[103]; dotted lines in left graph [3 & 7]) to illustrate the effect that half-life in brain can have on the resulting concentration distribution. Transferrin and lactoferrin (dashed lines in left graph [4 & 8]) are bilobal iron-binding proteins with very similar molecular weight (MW, 80 kDa) and d_H (~9 nm) but differ dramatically in their ability to bind heparan sulfate proteoglycans of the brain ECM (lactoferrin does bind while transferrin does not).[44] The $t_{1/2}$ for lactoferrin was estimated using the reported value for transferrin to illustrate how transient binding of lactoferrin to relatively fixed heparan sulfate sites along its diffusion path might retard the concentration distribution of lactoferrin relative to transferrin (D^* for lactoferrin is reduced, resulting in a steeper decline in concentration with distance). Other macromolecules may experience binding that further limits their distribution into the brain from the brain-CSF interface. Generally, concentration with distance declines more rapidly as molecules: (i) become larger (D^* decreases), (ii) experience additional sources of diffusional hindrance such as binding (D^* further decreases) or (iii) experience higher clearance from the brain (i.e. $t_{1/2}$ decreases).

Table 1

Diffusion data of selected substances at 37 °C [a]

Molecule	MW (kDa)	D ($\times 10^{-7}$ cm^2/s)	d_H (nm)[b]	D^* ($\times 10^{-7}$ cm^2/s)	tortuosity (λ)	$t_{1/2}$ (hr)[c]	k_e (1/hr) [c]	Notes	Source
Sucrose	0.342	70.0	0.90	31.0	1.50	2.62	0.26	dog cortex RT-VCP	50,83
Inulin	5	24.4	2.69	11.7	1.44	2.25	0.30	dog cortex RT-VCP	59,83
Dex3	3	22.2	2.95	5.36	2.04			rat cortex IOI *in vivo*	42
EGF	6.6	17.8	3.69	5.55	1.79			rat cortex IOI slice	68
NGF	26.5	13.5	4.86	2.95	2.14	1.20	0.57	rat striatum multiphoton slice	72
Lactalbumin	14.5	12.7	5.16	2.54	2.24			rat cortex IOI slice	67
Ovalbumin	45	10.7	6.12	1.71	2.50			rat cortex IOI slice	67
BSA	66	8.88	7.39	1.75	2.26	1.88 (12.2) [d]	0.36 (0.06) [d]	rat cortex IOI slice	67, 83,(104)
Transferrin	80	7.50	8.81	1.40	2.31	2.82	0.25	rat cortex IOI *in vivo*	44, 105
Lactoferrin	80	7.10	9.29	0.58	3.50			rat cortex IOI *in vivo*	44
Dex70	70	4.67	14.1	0.65	2.68	2.96 (15) [d]	0.23 (0.05) [d]	rat cortex IOI *in vivo*	42, 83,(103)
Quantum Dot	n/a	1.86	35.4	0.02	10.55			rat cortex IOI *in vivo*	42
PEG (ctx)	2	21.2	n/a	8.36	1.59			rat cortex IOI slice	69
PEG (str)	2	21.2	n/a	9.32	1.51			rat striatum IOI slice	69
PHPMA	28	6.75	n/a	2.46	1.66			rat cortex IOI slice	71
PHPMA	47	5.04	n/a	2.14	1.53			rat cortex IOI slice	71
PHPMA	220	2.14	n/a	0.78	1.66			rat cortex IOI slice	71
PHPMA	515	1.29	n/a	0.51	1.58			rat cortex IOI slice	71
PHPMA	1057	0.77	n/a	0.36	1.46			rat cortex IOI slice	71
PHPMA- BSA	176	2.46	n/a	0.48	2.26			rat cortex IOI slice	71

Footnotes: MW, molecular weight; D, free diffusion; d_H, hydrodynamic diameter; D^*, effective diffusion coefficient; $t_{1/2}$, half-life in brain; k_e, brain efflux constant; RT-VCP, radiotracer-ventriculocisternal perfusion method; IOI, integrative optical imaging; Dex3, 3 kDa dextran; EGF, epidermal growth factor; NGF, nerve growth factor; BSA, bovine serum albumin; Dex70, 70 kDa dextran; PEG, polyethylene glycol; PHPMA, poly[N-(2-hydroxypropyl)methacrylamide]; PHPMA-BSA, PHPMA and BSA conjugate; ctx, cortex; str, striatum.

[a] d_H calculated using the Stokes-Einstein equation: $D = (k_B T)/(3 \pi \eta d_H)$; k_B, Boltzman's constant; T, temperature in Kelvin; η, viscosity at a given temperature[68];

[b] All diffusion coefficients corrected to 37°C by multiplying by (T_{37} η_{temp})/(T_{temp} η_{37}) to facilitate direct comparison across substances; T_{37}, 310 K; η_{37}, viscosity of water at T_{37}; T_{temp}, temperature that diffusion measurements were made at in K; η_{temp}, viscosity of water at T_{temp}.

[c] The brain efflux constant, k_e, and related half-life in brain ($t_{1/2}$ = ln2/k_e) were calculated using the brain efflux index or related methods.[82,83]

[d] Examples of molecules with reported $t_{1/2}$ and k_e values with large variations as measured by different groups using similar methods.